

A MULTICHANNELED FILTER IN A PHOTONIC CRYSTAL CONTAINING COUPLED DEFECTS

H.-T. Hsu¹, M.-H. Lee², T.-J. Yang³, Y.-C. Wang², and C.-J. Wu^{2, *}

¹Department of Communications Engineering, Yuan-Ze University, Chungli 320, Taiwan, R.O.C.

²Institute of Electro-Optical Science and Technology, National Taiwan Normal University, Taipei 116, Taiwan, R.O.C.

³Department of Electrical Engineering, Chung Hua University, Hsinchu 300, Taiwan, R.O.C.

Abstract—Optical filtering properties in a multichanneled transmission filter based on one-dimensional photonic crystal containing the coupled defects are theoretically investigated. The resonant transmission peaks are designed to be located within the photonic band gap of a defect-free photonic crystal. The number of peaks is directly equal to the number of the coupled defects. The positions of resonant peaks can be tuned by varying the refractive index of the defect layer. In addition, extremely resonant peaks can be produced by adding the Bragg mirrors at the front and rear sides of the structure.

1. INTRODUCTION

With their unique ability to manipulate and control the light, photonic crystals (PCs) have been of much interest to the communities of photonics and condensed matter physics in the past two decades [1–4]. Due to the periodically arranged structures in PCs, there exist some photonic band gaps (PBGs), which are analogous to the electronic band gaps in solids. Electromagnetic waves with frequencies within PBGs are thus prohibited to propagate. PCs are also referred to as the PBG materials. Engineering PBG materials to realize the practical photonic devices are now available, including filters, polarizers, resonators, splitter, waveguides, and so on [5–20].

Received 14 May 2011, Accepted 9 June 2011, Scheduled 15 June 2011

* Corresponding author: Chien-Jang Wu (jasperwu@ntnu.edu.tw).

In a simple one-dimensional photonic crystal (1D PC), the structure is denoted as $\text{air}/(\text{AB})^N/\text{air}$ in which A and B are the high- and low-index layers, respectively, and N is the number of periods. By adding the defect layer to break the structurally periodic feature, a defect mode can be produced inside the PBG, and the defective PC is $\text{air}/(\text{AB})^M\text{C}(\text{AB})^M/\text{air}$ with a defect layer of C. This existing defect mode leads to a high transmittance in the frequency (or wavelength) domain, which can be used to design a narrowband transmission filter (NBTF) or simply a multilayer Fabry-Perot resonator (FPR). A simple and typical NBTF can be achieved by making use of the quarter-wavelength stacks, i.e., the optical lengths of the two constituents and defect satisfy $n_A d_A = n_B d_B = n_C d_C = \lambda_0/4$, where λ_0 is the design wavelength. In this case, two consecutive layers of AA or BB represent an absentee layer, and $(\text{AB})^M\text{C}(\text{AB})^M$ can be effectively reduced to a single layer of A or B, depending on C is taken to be A or B, respectively [21–23]. Such an NBTF only has a single resonant transmission peak at λ_0 , which locates in the PBG center. In addition, the peak shape can become much sharper as M increases. An extremely sharp peak, in turn, indicates a strongly localized defect mode that is produced due to the enhancement of the photonic confinement at a large M -number. In addition to Refs. [21–23] there have been other related studies on the NBTF [24–27].

As far as the applicational viewpoint is concerned, the presence of a single resonant peak within the PBG seems to be inefficient because much of the PBG bandwidth is wasted. To improve the spectral efficiency in utilizing the PBG, it is necessary to have a multichanneled transmission filter (MTF) with multiple resonant peaks inside the PBG. Indeed, Qiao et al., have first proposed a scheme to realize an MTF [28]. Instead of using a single defect layer C like in a defective PC like $\text{air}/(\text{AB})^N\text{C}(\text{AB})^N/\text{air}$, they use the photonic quantum well (PQW) as a defect such that the structure of MTF becomes $\text{air}/(\text{AB})^N(\text{CD})^M(\text{AB})^N/\text{air}$ where the PQW is represented by $(\text{CD})^M$ with $M < N$. In addition, the PQW constituents C and D are different from A and B.

In principle, the MTF, $\text{air}/(\text{AB})^N(\text{CD})^M(\text{AB})^N/\text{air}$ is designed to let the pass band of the PC, $(\text{CD})^M$, be located within one of the PBGs of the host PC, $(\text{AB})^N$. With the photonic confinement between two Bragg mirrors $(\text{AB})^N$, the confined continuous pass band is then quantized and consequently nearly discrete modes are created with number of quantized modes being equal to M , the number of periods of the PQW. Thus, the refractive indices and the thicknesses of C and D must be appropriately chosen to cause the pass band to be completely located within the band gap of the host PC. This could be a strict

condition and limits the flexibility of design. There have been many reports on the MTFs based on the PQW [29–32].

To avoid the strict condition of using PQW in realizing an MTF, another version of defective PC that can also work as an MTF is proposed [33]. In this design, the original defect-free PC, $\text{air}/(\text{AB})^N\text{A}/\text{air}$, is modified as $\text{air}/(\text{ABAC})^N\text{ABA}/\text{air}$, in which some of the low-index layers, B's are replaced by C's called the impurity or defect layers. With the insertion of C's, impurity bands can be produced within the PBG of the original PC, $\text{air}/(\text{AB})^N\text{A}/\text{air}$. The appearance of such impurity bands is analogous to that in the doped semiconductor. Thus, the structure, $\text{air}/(\text{ABAC})^N\text{ABA}/\text{air}$, can function as an MTF with number of defect modes equal to N , the number of the coupled defect layers. Although the goal of MTF can be reached in this design, the resonant peaks are not so sharp as those in $\text{air}/(\text{AB})^N(\text{CD})^M(\text{AB})^N/\text{air}$. To make the peaks as sharp as possible, the structure is sandwiched by two Bragg mirrors, i.e., $\text{air}/(\text{AB})^M(\text{ABAC})^N\text{ABA}(\text{BA})^M/\text{air}$. This MTF can thus be used as a frequency-selective device which is of technical use in communications.

In this paper, we give a more detailed analysis on the tunable optical filtering properties in this type MTF based on the use of impurity. We vary the refractive index of the impurity layer and see how the resonant peaks move as a function of the defect index. We also study modified version of this MTF, $\text{air}/(\text{ABCB})^N\text{ABA}/\text{air}$, namely some of the high-index layers A's are replaced with the defect layers C's. A different tunable feature will be seen when A or B is replaced by C. Additionally, the dependence of tunability on whether N is an even or odd number will also be elucidated.

2. BASIC EQUATIONS

To investigate the tunable properties of the impurity-based MTF, transfer matrix method (TMM) developed by Yeh will be used to calculate the transmittance T , which is expressed as $T = |t|^2$, where t is the transmission coefficient [34]. According to TMM, in an N -layer structure, $\text{air}/1/2/3/\dots/N/\text{air}$ (The left "air" is called the start medium whereas the right one is the stop medium) the total transfer matrix is given by

$$\mathbf{M} = \begin{pmatrix} m_{11} & m_{12} \\ m_{21} & m_{22} \end{pmatrix} = \mathbf{D}_0^{-1} (\mathbf{M}_1 \mathbf{M}_2 \dots \mathbf{M}_N) \mathbf{D}_0, \quad (1)$$

where the transfer matrix \mathbf{M}_i for layer i is written as

$$\mathbf{M}_i = \mathbf{D}_i \mathbf{P}_i \mathbf{D}_i^{-1}, \quad i = 1, 2, \dots, N. \quad (2)$$

Here, the dynamical matrix \mathbf{D}_i for medium i related to its refractive index n_i is

$$\mathbf{D}_i = \begin{pmatrix} 1 & 1 \\ n_i & -n_i \end{pmatrix}, \quad i = 0, 1, 2, \dots, N, \quad (3)$$

where $i = 0$ means the air with $n_0 = 1$, and the translational matrix \mathbf{P}_i in each layer i is expressible as

$$\mathbf{P}_i = \begin{pmatrix} \exp(jk_0 n_i d_i) & 0 \\ 0 & \exp(-jk_0 n_i d_i) \end{pmatrix}, \quad i = 1, 2, \dots, N, \quad (4)$$

where d_i is the corresponding thickness and $k_0 = \omega/c$ is the wave number in free space, where c is the speed of light in vacuum. Here, we are only interested in the case of normal incidence and have adopted the convention $\exp(j\omega t)$ for the temporal part in all fields.

With the available matrix elements in Equation (1), the transmission coefficient t is calculated to be

$$t = \frac{1}{m_{11}}. \quad (5)$$

As a result, the transmittance is

$$T = \left| \frac{1}{m_{11}} \right|^2. \quad (6)$$

If the start and stop media are different, say a substrate of index n_s is the stop medium, then the transmittance must be written as

$$T = \frac{n_s}{n_0} \left| \frac{1}{m_{11}} \right|^2. \quad (7)$$

3. ANALYTICAL RESULTS AND DISCUSSION

Figure 1 shows the calculated transmittance for a defect-free host PC of air/(AB)^NA/air. Here, $N = 4, 8, 16$, and 32 are taken for the purpose of comparison. It is seen that a standard U-shape PBG with center at ω_0 is generated for $N = 32$. In fact, based on the theory of Bragg reflector, both the left and right band edges, ω_L and ω_R , can be exactly determined as follows [21]:

$$\omega_L = 2c \frac{\cos^{-1}(\rho)}{n_H d_H + n_L d_L}, \quad \omega_R = 2c \frac{\cos^{-1}(-\rho)}{n_H d_H + n_L d_L}, \quad (8)$$

where $\rho = (n_1 - n_2)/(n_1 + n_2)$ is the Fresnel reflection coefficient. The calculated results are $\omega_L/\omega_0 = 0.891$ and $\omega_R/\omega_0 = 1.109$. Thus, the PBG center ω_c is exactly at the design frequency ω_0 because

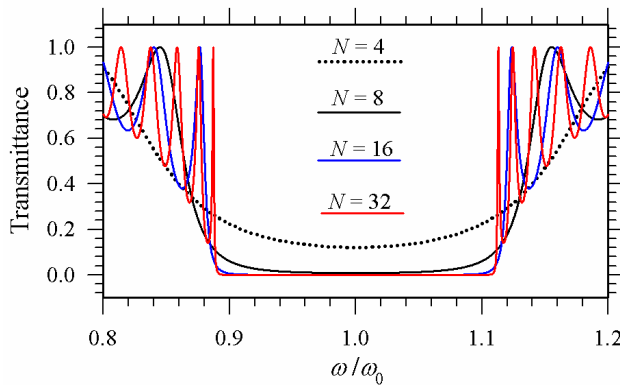


Figure 1. Calculated frequency-dependent transmittance for defect-free host photonic crystal of air/(AB)^NA/air at different numbers of periods of $N = 4, 8, 16$, and 32 . The center wavelength is designed at $\lambda_0 = 500$ nm such that $\omega_0 = 2\pi c/\lambda_0$.

$\omega_c/\omega_0 = (\omega_L/\omega_0 + \omega_R/\omega_0)/2 = 1$. All these results agree with those shown in Figure 1 for $N = 32$.

In what follows we shall present the analytical results for the transmittance as a function of the frequency for the impurity-based MTF. The first structure to be considered is air/(ABAC)^NABA/air (structure-I). Without loss of generality, we take the refractive indices for layers A and B as $n_1 = 1.41$ and $n_2 = 1$, respectively [33]. In addition, both A and B are taken to be quarter-wavelength layers, i.e., $n_1 d_1 = n_2 d_2 = \lambda_0/4$, where the design wavelength is $\lambda_0 = 500$ nm. The design frequency is then given by $\omega_0 = 2\pi c/\lambda_0 = 2\pi \times 6 \times 10^{14}$ rad/s. The impurity layer C is taken to be a half-wavelength layer of $n_3 d_3 = \lambda_0/2$, where $n_3 = n_2 = 1$ will be used.

With the PBG in Figure 1, we are now in a position to engineer it to realizing an MTF by adding the defect or impurity bands. Figure 2 shows the first design of structure-I, air/(ABAC)^NABA/air, where the low-index layer B (quarter-wave layer) is replaced by a defect C (half-wave layer). It can be from Figure 2 that the number of peaks is equal to N , the number of coupled defects. The resonant peaks are symmetrically distributed about gap center at $\omega_c/\omega_0 = 1$. For $N = \text{odd}$, the center of PBG, $\omega_c/\omega_0 = 1$, is a resonant peak frequency, while it is not a resonant peak frequency when $N = \text{even}$. Since C is a half-wave layer with the same refractive index as B, i.e., $C = BB$ and since two consecutive AA or BB becomes an absentee layer,

the whole structure, $(ABAC)^N ABA$, will reduce to an absentee layer at $\omega_c/\omega_0 = 1$ for $N = \text{odd}$, leading to a complete transmission (total transparency) because the impedance of the whole structure is matched with that of air. However, it will reduce to ABA at $\omega_c/\omega_0 = 1$ for $N = \text{even}$. As a result, at the center point, no transmission peak is found and, in fact, it becomes a dip, as shown in Figure 2.

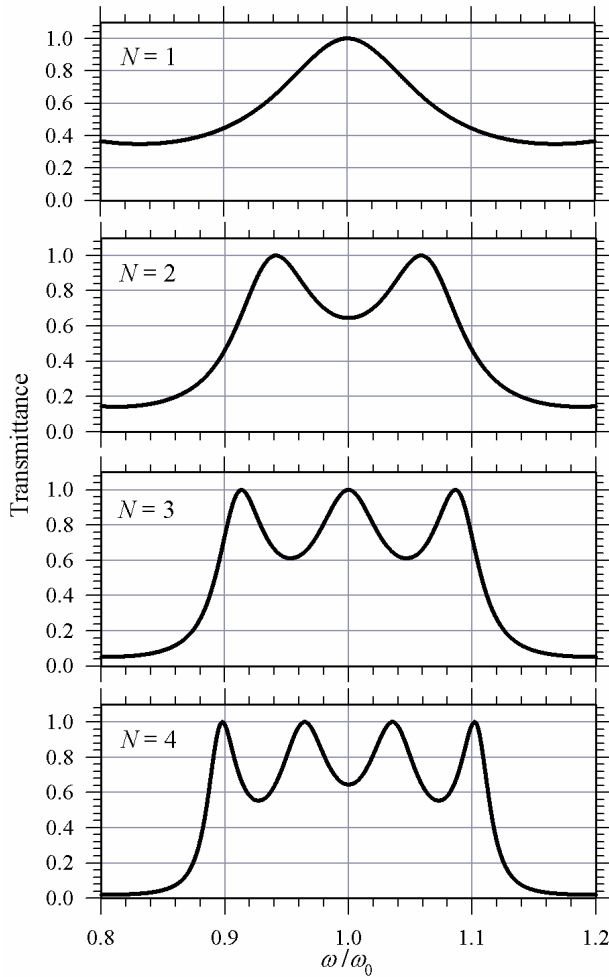


Figure 2. Calculated frequency-dependent transmittance for a defective photonic crystal (structure-I), air/ $(ABAC)^N ABA$ /air, at $N = 1, 2, 3$, and 4 , respectively. For a fixed value of N , the number of transmittance peaks is found to be equal to N for N coupled defects.

Let us now vary the refractive index n_3 of defect C in structure-I of $(ABAC)^N ABA$ and keep its optical length the same as $\lambda_0/2$. In Figure 3, the shifting properties in the resonant peaks at distinct values of $n_3 = 1, 1.2, 1.4, 1.6, 1.8$, and 2.0 are illustrated for $N = 3$ (left panel) and $N = 4$ (right panel), respectively. It is seen that position of the peak (for $N = 3$) or dip (for $N = 4$) at PBG center $\omega_c/\omega_0 = 1$ remains unchanged as n_3 changes. However, when n_3 increases we find that the peaks to the left of center are moved to the lower frequencies and those at the right side of center are shifted to the higher frequencies. At $N = 4$, the four peak frequencies are labeled as $\omega_1, \omega_2, \omega_3$, and ω_4 . The shifting behavior is at ω_1 and ω_4 is more pronounced than ω_2 and ω_3 . The shift in these four peak frequencies versus the defect index is plotted in Figure 4. The separation between two adjacent peaks is appreciably increased as the defect index increases.

The shift in the resonant frequencies due to the variation of defect index can be qualitatively argued as follows: At resonant transmission each defect C can be regarded as a cavity resonator. When they are coupled together to form a multichanneled filter, interactions between these coupled defects will be created such that the resonant frequencies are shifted at different values of refractive. In structure-I, the two adjacent defects are separated by ABA, which is effectively like a “potential barrier” with respect to the defects. This barrier causes

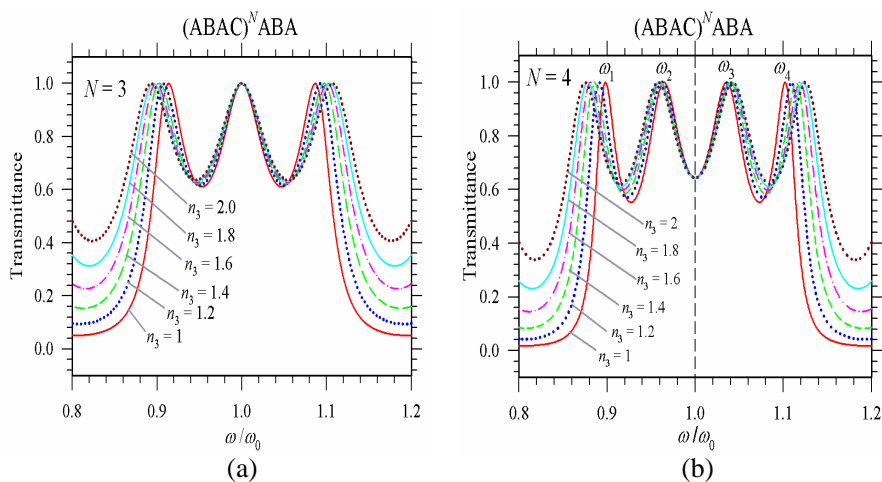


Figure 3. Calculated frequency-dependent transmittance for a defective photonic crystal (structure-I), air/ $(ABAC)^N$ ABA/air, at (a) $N = 3$ (left panel), and (b) $N = 4$ (right panel), respectively, for different refractive indices of defect C.

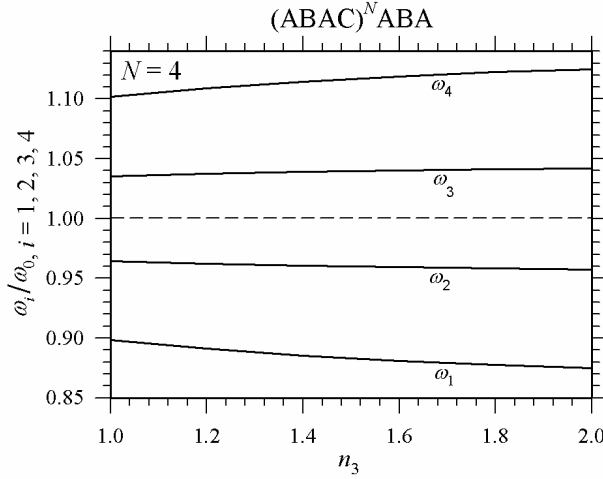


Figure 4. Calculated peak frequencies as a function of the refractive index of the defect C for the filter of structure-I, air/(ABAC)^NABA/air with $N = 4$.

a repulsive interaction between the defects. With the increase in the defect index, the physical thickness of defect will be reduced because we fixed its optical thickness at $\lambda_0/2$. For $N = \text{odd}$ (e.g., 3), the resultant interaction in the center defect is canceled by the two adjacent defect, leading to the independence of the different indices. For the left or right defect, the net interaction becomes stronger at a reduced thickness. As a result, the resonant frequency higher than center frequency will become even higher, and the resonant frequency lower than center frequency will become even lower, as illustrated in Figure 3. This is similar to the “repulsive interaction” in quantum mechanics. Similar argument can be valid for $N = \text{even}$. A possible detailed analysis can be made by making use of the tight binding method [35], which is obviously beyond the scope of the current study.

We continue to engineer the PBG of the host PC to obtaining an MTF by replacing the high-index layer A by the defect C, i.e., air/(ABCB)^NABA/air, which is now referred to as structure-II. In this case, the number peaks is also equal to N . Figure 5 depicts the frequency-dependent transmittance for $N = 4$ at different defect index of $n_3 = 1.41, 1.61, 1.81, 2.01, 2.21$, and 2.41 . It is of interest to see that the shifting trend in the peak frequencies is opposite to that in right panel of Figure 3, except at the center frequency, $\omega_c/\omega_0 = 1$. The peak frequencies as a function of n_3 are plotted in Figure 6.

The shifting behavior in the resonant frequencies can be similarly

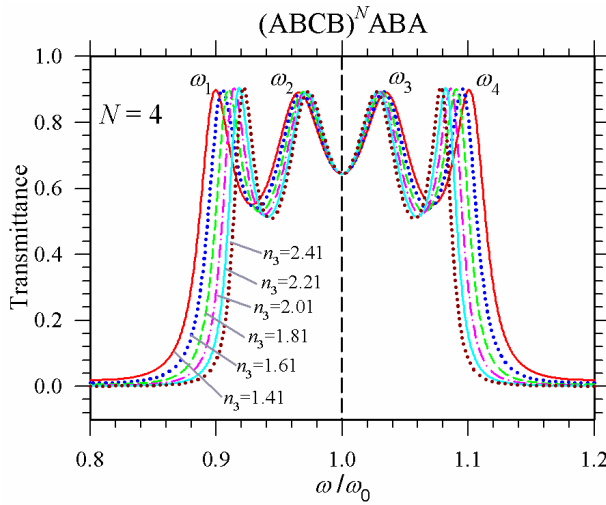


Figure 5. Calculated frequency-dependent transmittance for the filter of structure-II, air/(ABCB)^NABA/air, at $N = 4$ and different refractive indices of defect C.

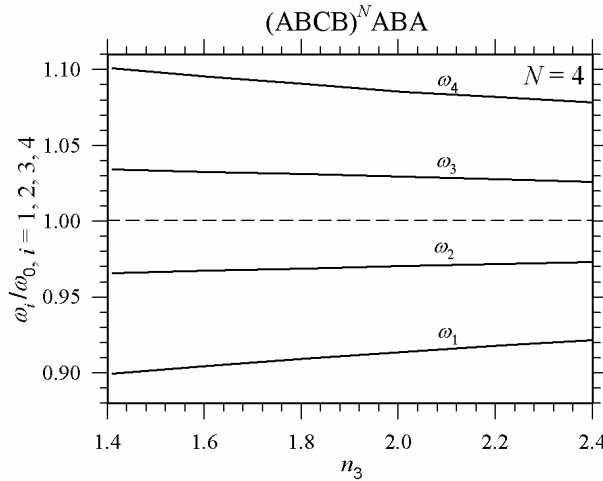


Figure 6. Calculated peak frequencies as a function of the refractive index of the defect C for the filter of structure-II, air/(ABCB)^NABA/air with $N = 4$.

argued as in Figures 3 and 4. However, in structure-II, the interaction between the defects will be the “attractive interaction” because the defects are separated by BAB, which effectively acts as “potential

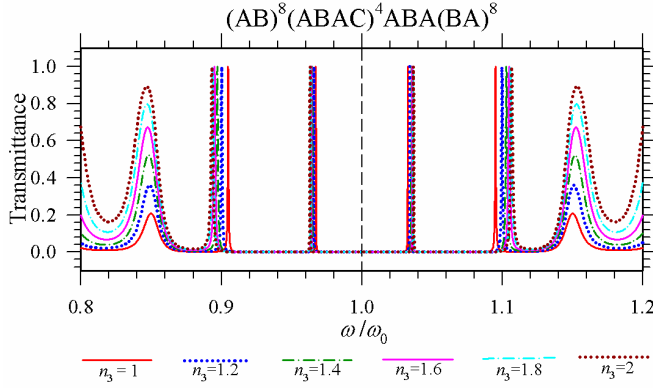


Figure 7. Calculated frequency-dependent transmittance for the structure-I with mirrors, $\text{air}/(\text{AB})^8(\text{ABAC})^4\text{ABA}(\text{BA})^8/\text{air}$, at different refractive indices of defect C.

well” with respect to the defects. With such interaction, the resonant frequency higher than center frequency will be decreased, and the resonant frequency lower than center frequency will be increased, as illustrated in Figure 4. Thus, the shifting trend in structure-II is opposite to that in structure-I.

In Figure 7, we plot the transmittance spectra for the structure-I confined by two Bragg mirrors, i.e., we have a defective PC like $\text{air}/(\text{AB})^M(\text{ABAC})^N\text{ABA}(\text{BA})^M/\text{air}$ with $M = 8$, $N = 4$ being used. With the addition of two mirrors, the photonic confinement is greatly enhanced, which, in turn, causes the resonant peaks shown in right panel of Figure 3 to be strongly located, as shown in Figure 7. In addition, the confinement effect also enhances the bands outside the PBG. The transmittance of the side bands is significantly increased at a larger index of the defect layer. The dependence of shifting behavior on the defect index is similar to the right panel of Figure 3.

Before entering into the conclusion, let us make some brief comments on the above results. First, the above resonant frequency tuning feature is made based on the variation of the refractive index of the defect layer. From a practical point of view, it would be difficult to vary the refractive index so widely with impurity doping. Other methods, such as changing the defect layer thickness, may be more suitable for the resonant frequency tuning. This is because the tuning is closely related to the optical thickness in the defect layer. Thus, either changing in refractive index or thickness can achieve the goal. Second, both structure-I and structure-II can be used to fulfill the multichanneled filtering property, only the different tuning trend as

a function of the refractive index. Thus, the advantages of these two structures are expected to be equally taken. In addition, similar spectrum as in Figure 7 (the structure-I with Bragg mirrors) can be obtained for the structure-II by adding the Bragg mirrors.

4. SUMMARY

By engineering the impurity or defect band in the PBG with coupled impurities in a quarter-wavelength stack, a multichanneled transmission filter can be achievable. The optically filtering properties in such a filter have been investigated. The number of defect modes is equal to the number of coupled impurity (or defect) layers. At the PBG center, there is a resonant peak in transmittance when N is odd, but it is not as N is even. It is shown that positions of the resonant peaks can be tuned by varying the index of the impurity layer. The shifting trend has been illustrated for both cases where the impurity layer is in place of the high- or low-index layer. The effect of strong confinement coming from the Bragg mirrors is also demonstrated.

ACKNOWLEDGMENT

C.-J. Wu acknowledges the financial support from the National Science Council of the Republic of China (Taiwan) under Contract No. NSC-97-2112-M-003-013-MY3.

REFERENCES

1. Yablonovitch, E., "Inhibited spontaneous emission in solid state physics and electronics," *Phys. Rev. Lett.*, Vol. 58, 2059–2062, 1987.
2. John, S., "Strong localization of photons in certain disordered lattices," *Phys. Rev. Lett.*, Vol. 58, 2486–2489, 1987.
3. Joannopoulos, J. D., R. D. Meade, and J. N. Winn, *Photonic Crystals: Molding the Flow of Light*, Princeton University Press, Princeton, NJ, 1995.
4. Guida, G., A. de Lustrac, and A. Priou, "An introduction to photonic band gap (PBG) materials," *Progress In Electromagnetics Research*, Vol. 41, 1–20, 2003.
5. Lin, W.-H., C.-J. Wu, T.-J. Yang, and S.-J. Chang, "Terahertz multichanneled filter in a superconducting photonic crystal," *Optics Express*, Vol. 18, 27155–27166, 2010.

6. Shen, W., X. Sun, Y. Zhang, Z. Luo, X. Liu, and P. Gu, "Narrow band filter in both transmission and reflection with metal/dielectric thin films," *Optics Communication*, Vol. 282, 242–246, 2009.
7. Sun, X. Z., P. F. Gu, W. D. Shen, X. Liu, Y. Wang, and Y. G. Zhang, "Design and fabrication of a novel reflection filter," *Applied Optics*, Vol. 46, 2899–2902, 2007.
8. Ye, Y.-H., J. Ding, D.-Y. Jeong, I. C. Khoo, and Q. M. Zhang, "Finite-size effect on one-dimensional coupled-resonator optical waveguides," *Phys. Rev. E*, Vol. 69, 056604, 2004.
9. Nelson, R. L. and J. W. Haus, "One-dimensional photonic crystals in reflection geometry for optical applications," *Appl. Phys. Lett.*, Vol. 83, 1089–1091, 2003.
10. Fink, Y., J. N. Winn, S. Fan, C. Chen, J. Michel, J. D. Joannopoulos, and L. E. Thomas, "A dielectric omnidirectional reflector," *Science*, Vol. 282, 1679–1682, 1998.
11. Li, H. and X. Yang, "Larger absolute band gaps in two-dimensional photonic crystals fabricated by a three-order-effect method," *Progress In Electromagnetics Research*, Vol. 108, 385–400, 2010.
12. Wu, C.-J., J.-J. Liao, and T. W. Chang, "Tunable multilayer Fabry-Perot resonator using electro-optical defect layer," *Journal of Electromagnetic Waves and Applications*, Vol. 24, No. 4, 531–542, 2010.
13. Rahimi, H., A. Namdar, S. Roshan Entezar, and H. Tajalli, "Photonic transmission spectra in one-dimensional fibonacci multilayer structures containing single-negative metamaterials," *Progress In Electromagnetics Research*, Vol. 102, 15–30, 2010.
14. Chen, D., M.-L. Vincent Tse, and H.-Y. Tam, "Optical properties of photonic crystal fibers with a fiber core of arrays of subwavelength circular air holes: Birefringence and dispersion," *Progress In Electromagnetics Research*, Vol. 105, 193–212, 2010.
15. Nozhat, N. and N. Granpayeh, "Specialty fibers designed by photonic crystals," *Progress In Electromagnetics Research*, Vol. 99, 225–244, 2009.
16. Shi, Y., "A compact polarization beam splitter based on a multimode photonic crystal waveguide with an internal photonic crystal section," *Progress In Electromagnetics Research*, Vol. 103, 393–401, 2010.
17. Choudhury, P. K. and W. K. Soon, "TE mode propagation through tapered core liquid crystal optical fibers," *Progress In*

- Electromagnetics Research*, Vol. 104, 449–463, 2010.
18. Qi, L.-M. and Z. Yang, “Modified plane wave method analysis of dielectric plasma photonic crystal,” *Progress In Electromagnetics Research*, Vol. 91, 319–332, 2009.
 19. Sabah, C. and S. Uckun, “Multilayer system of lorentz/drude type metamaterials with dielectric slabs and its application to electromagnetic filters,” *Progress In Electromagnetics Research*, Vol. 91, 349–364, 2009.
 20. Fu, X., C. Cui, and S. C. Chan, “Optically injected semiconductor laser for photonic microwave frequency mixing in radio-over-fiber,” *Journal Electromagnetic Waves and Applications*, Vol. 24, No. 7, 849–960, 2010.
 21. Orfanidis, S. J., *Electromagnetic Waves and Antennas*, No. 7, Rutgers University, 2008, www.ece.rutgers.edu/~orfanidi/ewa.
 22. Smith, D. R., R. Dalichaouch, N. Kroll, S. Schultz, S. L. McCall, and P. M. Platzman, “Photonic band structure without and with defect in one-dimensional photonic crystal,” *J. Opt. Soc. Am. B: Optical Physics*, Vol. 10, 314–321, 1993.
 23. Wu, C.-J. and Z.-H. Wang, “Properties of defect modes in one-dimensional photonic crystals,” *Progress In Electromagnetics Research*, Vol. 103, 169–184, 2010.
 24. Hsu, H.-T. and C.-J. Wu, “Design rules for a Fabry-Perot narrow band transmission filter containing a metamaterial negative-index defect,” *Progress In Electromagnetics Research Letters*, Vol. 9, 101–107, 2009.
 25. Smolyakov, A. I., E. A. Fourkal, S. I. Krashenninnikov, and N. Sternberg, “Resonant modes and resonant transmission in multi-layer structures,” *Progress In Electromagnetics Research*, Vol. 107, 293–314, 2010.
 26. Hsu, H.-T., T.-W. Chang, T.-J. Yang, B.-H. Chu, and C.-J. Wu, “Analysis of wave properties in photonic crystal narrowband filters with left-handed defect,” *Journal of Electromagnetic Waves and Applications*, Vol. 24, No. 16, 2285–2298, 2010.
 27. Wang, J., S. Qu, H. Ma, J. Hu, Y. Yang, X. Wu, Z. Xu, and M. Hao, “A dielectric resonator-based route to left-handed metamaterials,” *Progress In Electromagnetics Research B*, Vol. 13, 133–150, 2009.
 28. Qiao, F., C. Zhang, and J. Wan, “Photonic quantum-well structure: Multiple channeled filtering phenomena,” *Appl. Phys. Lett.*, Vol. 77, 3698–3700, 2000.
 29. Liu, J., J. Sun, C. Huang, W. Hu, and D. Huang, “Optimizing the

- spectral efficiency of photonic quantum well structures,” *Optik*, Vol. 120, 35–39, 2009.
30. Liu, J., J. Sun, C. Huang, W. Hu, and M. Chen, “Improvement of spectral efficiency based on spectral splitting in photonic quantum-well structures,” *IET Optoelectron.*, Vol. 2, 122–127, 2008.
 31. Feng, C. S., L. M. Mei, L. Z. Cai, P. Li, and X. L. Yang, “Resonant modes in quantum well structure of photonic crystals with different lattice constants,” *Solid State Communications*, Vol. 135, 330–334, 2005.
 32. Haxha, S., W. Belhadj, F. Abdelmalek, and H. Bouchriha, “Analysis of wavelength demultiplexer based on photonic crystals,” *IEE Proc. Optoelectron.*, Vol. 152, 193–198, 2005.
 33. Jiang, H. T., H. Chen, N.-H. Liu, and S.-Y. Zhu, “Engineering photonic crystal impurity bands for multiple channeled optical switches,” *Chin. Phys. Lett.*, Vol. 21, 101–103, 2004.
 34. Yeh, P., *Optical Waves in Layered Media*, John Wiley & Sons, Singapore, 1998.
 35. Markos, P. and C. M. Soukoulis, *Wave Propagation: From Electrons to Photonic Crystals*, Princeton University Press, New Jersey, 2008.